

Article

Comparative Analysis of CAZymes from *Trichoderma longibrachiatum* LMBC 172 Cultured with Three Different Carbon Sources: Sugarcane Bagasse, Tamarind Seeds, and Hemicellulose Simulation

Alex Graça Contato ^{1,2,*}, Tiago Cabral Borelli ³, Ana Karine Furtado de Carvalho ⁴, Heitor Buzetti Simões Bento ⁵, Marcos Silveira Buckeridge ⁶, Janet Rogers ⁷, Steven Hartson ⁷, Rolf Alexander Prade ² and Maria de Lourdes Teixeira de Moraes Polizeli ^{1,8}

- ¹ Department of Biochemistry and Immunology, Faculty of Medicine of Ribeirão Preto, University of São Paulo, Ribeirão Preto 14040-900, SP, Brazil; polizeli@ffclrp.usp.br
 - ² Department of Microbiology and Molecular Genetics, Oklahoma State University, Stillwater, OK 74078, USA; rolf.prade@okstate.edu
 - ³ Department of Cellular and Molecular Biology and Pathogenic Bioagents, Faculty of Medicine of Ribeirão Preto, University of São Paulo, Ribeirão Preto 14040-900, SP, Brazil; tiago.borelli@usp.br
 - ⁴ Department of Basic and Environmental Sciences, Lorena School of Engineering, University of São Paulo, Lorena 12602-810, SP, Brazil; anacarvalho@usp.br
 - ⁵ Department of Bioprocess Engineering and Biotechnology, School of Pharmaceutical Sciences, São Paulo State University, Araraquara 14800-903, SP, Brazil; heitor.bento@unesp.br
 - ⁶ Department of Botany, Institute of Biosciences, University of São Paulo, São Paulo 05508-090, SP, Brazil; msbuck@usp.br
 - ⁷ Department of Biochemistry and Molecular Biology, Oklahoma State University, Stillwater, OK 74078, USA; janet.rogers@okstate.edu (J.R.); hartson.steve@gmail.com (S.H.)
 - ⁸ Department of Biology, Faculty of Philosophy, Sciences and Letters of Ribeirão Preto, University of São Paulo, Ribeirão Preto 14040-900, SP, Brazil
- * Correspondence: alexgraca.contato@gmail.com



Citation: Contato, A.G.; Borelli, T.C.; de Carvalho, A.K.F.; Bento, H.B.S.; Buckeridge, M.S.; Rogers, J.; Hartson, S.; Prade, R.A.; Polizeli, M.d.L.T.d.M. Comparative Analysis of CAZymes from *Trichoderma longibrachiatum* LMBC 172 Cultured with Three Different Carbon Sources: Sugarcane Bagasse, Tamarind Seeds, and Hemicellulose Simulation. *Clean Technol.* **2024**, *6*, 994–1010. <https://doi.org/10.3390/cleantechnol6030050>

Academic Editor: Patricia Luis Alconero

Received: 6 June 2024

Revised: 24 July 2024

Accepted: 5 August 2024

Published: 8 August 2024



Copyright: © 2024 by the authors. Licensee MDPI, Basel, Switzerland. This article is an open access article distributed under the terms and conditions of the Creative Commons Attribution (CC BY) license (<https://creativecommons.org/licenses/by/4.0/>).

Abstract: The examination of fungal secretomes has garnered attention for its potential to unveil the repertoire of secreted proteins, notably CAZymes (Carbohydrate-Active enzymes), across various microorganisms. This study presents findings on categorizing the secretome profile of CAZymes by their function and family, derived from the filamentous fungus *Trichoderma longibrachiatum* LMBC 172. The cultivation was performed through submerged fermentation with three distinct carbon sources: sugarcane bagasse, tamarind seeds, and a control simulating hemicellulose containing 0.5% beechwood xylan plus 0.5% oat spelt xylan. The secretome analysis revealed 206 distinct CAZymes. Each carbon source showed particularities and differences. Of these, 89 proteins were produced simultaneously with all the carbon sources; specifically, 41 proteins using only the hemicellulose simulation, 29 proteins when sugarcane bagasse was used as a carbon source, and only 3 when tamarind seeds were used. However, in this last condition, there was a high intensity of xyloglucanase GH74 production, thus reaffirming the richness of xyloglucan in the constitution of these seeds. When evaluating the proteins found in two conditions, 18 proteins were shown between the simulation of hemicellulose and sugarcane bagasse, 11 proteins between the simulation of hemicellulose and tamarind seeds, and 15 proteins between sugarcane bagasse and tamarind seeds. Among the proteins found, there are representatives of different families such as glycosyl hydrolases (GHs) that cleave cellulose, hemicellulose, pectin, or other components; carbohydrate esterases (CEs); polysaccharide lyases (PLs); carbohydrate-binding modules (CBMs); and auxiliary activity enzymes (AAs). These results demonstrate the importance of analyzing CAZymes secreted by microorganisms under different culture conditions.

Keywords: CAZymes; secretome; *Trichoderma longibrachiatum*; sugarcane bagasse; tamarind seeds

1. Introduction

The rise in agro-industrial operations has resulted in the accumulation of substantial quantities of lignocellulosic residues sourced from diverse origins, including wood and various agricultural byproducts globally [1–3]. Annually, approximately 146 billion tons of waste are generated worldwide [4]. There has been a notable surge in economic interest in these residues in recent years due to their renewability and cost-effectiveness, offering substantial potential for chemical and bioenergy production, such as bioethanol [5–7].

Plant biomass is composed of intricately structured polymeric materials, including proteins, lignin, hemicellulose (a composite of cellulose fibers enveloped in hemicellulose-pectin), ash, salts, and minerals [8,9]. The polysaccharide framework within the plant cell wall represents one of the most intricate structures, with its lignocellulosic constitution varying depending on its source [10,11]. These cell wall polysaccharides serve as energy reservoirs, which, upon efficient extraction, can be utilized to produce second-generation ethanol, particularly through the hydrolysis of sugarcane bagasse [12].

The process of converting lignocellulosic biomass into ethanol and other chemical compounds often relies on a multienzyme system that operates synergistically [5,13,14]. It is crucial to investigate various microorganisms and comprehend how they secrete enzymes relevant to these processes [15]. Consequently, examining the secretomes of various fungi has garnered attention. These studies offer insights into the secreted proteins, notably the CAZymes (Carbohydrate-Active enzymes), released by diverse microorganisms cultivated under different conditions [16–19]. CAZymes encompass numerous enzyme protein families, each classified based on protein sequence similarities and distinctive three-dimensional folding structures [20]. They are classified between glycosyl hydrolases (GHs) that cleave cellulose, hemicellulose, pectin, or other components; carbohydrate esterases (CEs); polysaccharide lyases (PLs); carbohydrate-binding modules (CBMs); and auxiliary activity enzymes (AAs). These analyses allow a better understanding of the ideal way to obtain proteins of industrial interest, in addition to enabling the discovery of proteins not yet described in the literature for the studied microorganisms [21].

One particularly intriguing microorganism is *Trichoderma longibrachiatum*, especially in the context of biotechnology and biomass bioconversion. *T. longibrachiatum* is distributed globally, with a predominant presence in warmer climates. Its colonies usually exhibit an initial off-white colony, which later transitions to a shade of greyish green with age [22]. The members of this clade have gained significant attention across different sectors due to their remarkable capacity to excrete substantial quantities of proteins and metabolites [23,24]. The enzymes produced by *T. longibrachiatum* are used in various industries, including food, beverages, textiles, and paper, due to their ability to degrade complex plant polysaccharides [25,26]. Additionally, some strains of *Trichoderma*, including *T. longibrachiatum*, are used as biocontrol agents, antagonizing plant pathogens and offering an eco-friendly alternative to chemical pesticides [27,28]. The study of the CAZymes from the secretome of *T. longibrachiatum* provides valuable insights into the molecular mechanisms of enzyme production and adaptation to different carbon sources, essential for engineering more efficient strains and understanding their ecological interactions. *T. longibrachiatum* can grow on a variety of substrates, including agro-industrial residues like sugarcane bagasse and tamarind seeds, making it an ideal model for biomass bioconversion studies and the development of sustainable biotechnological processes [23,26,29,30]. Moreover, the use of *T. longibrachiatum* in the degradation of agricultural residues not only adds value to these residues but also helps reduce the environmental impact associated with their improper disposal.

Sugarcane (*Saccharum* sp.) is classified as a monocotyledonous grass [31,32], with Brazil currently holding the title of the world's largest sugarcane producer, primarily concentrated in the central-southern region of the country [33]. Following Brazil, other significant sugarcane-producing countries include India, China, Thailand, and Pakistan. In 2022, global sugarcane production reached a total of 1.92 billion tons, with Brazil producing 38% of the world total, India with 23%, and China producing 5%. These values make it the third-most produced commodity worldwide [34]. Therefore, given that each ton

of sugarcane results in approximately 270 kg of bagasse, the global sugarcane crop in 2022 generated more than 500 million tons of bagasse. This significant quantity highlights the necessity of utilizing this abundant byproduct in countries with extensive sugarcane production [35]. Characterized by a secondary cell wall, sugarcane bagasse typically comprises approximately 32–45% cellulose, 20–32% hemicellulose, 17–32% lignin, and 1–9% ash, along with other constituents [36–38].

On the other hand, tamarind (*Tamarindus indica* L.) is a tropical fruit tree indigenous to equatorial Africa, India, and Southeast Asia, featuring both pulp and seeds encased in a tough shell [39]. The biggest tamarind producers in the world are countries such as India, Malaysia, Myanmar, Bangladesh, Sri Lanka, Thailand, the United Arab Emirates, and South American countries. When processing 1 kg of fresh tamarind, it will give 55% pulp, 30–40% seed, 6% peel, and 5% fiber. The seed is the main and underutilized byproduct of the tamarind pulp industry and contains approximately (70%) kernel and (30%) hard brown testa [40–42]. The processing techniques, particularly the removal of pulp from the pod or seeds from the pulp, as well as the handling and storage of the seed and pulp, are traditionally practiced in the growing region or country. However, the most common processing method involves completely removing the testa from the kernel. The testa is separated from the kernels either by roasting or by soaking the seeds in water. Given that the mineral content of the seed coat is higher than that of the cotyledon, it is expected that their thermal properties and behaviors differ, resulting in varying degrees of expansion and contraction. This difference aids in detaching the seed coat from the seed [42]. According to Gonçalves et al. [43], tamarind seed composition includes approximately $1.82 \pm 0.01\%$ ash, $33.07 \pm 1.40\%$ lignin, $33.31 \pm 3.56\%$ cellulose, and $10.45 \pm 1.45\%$ hemicellulose. Additionally, these seeds boast a significant xyloglucan content, accounting for roughly 40% of their dry mass [44], making them a promising resource for CAZymes exploration.

Due to their composition, sugarcane bagasse and tamarind seeds have been employed in cultivating microorganisms to generate microbial enzymes capable of breaking down lignocellulosic biomass [2,19,24,26,45]. In this context, the present study unveils the categorization of CAZymes by function and family within the secretome profile of the filamentous fungus *T. longibrachiatum* LMBC 172. The fungus was cultured via submerged fermentation with three distinct carbon sources: sugarcane bagasse, or tamarind seeds, or a control simulating hemicellulose. The hemicellulose simulation was chosen to be used because hemicellulose is the part of lignocellulose that needs a larger framework of enzymes for degradation [46]. The global annual production of hemicellulose is approximately 60 billion tons, making it the second-most abundant renewable component of lignocellulosic biomass, after cellulose [47].

2. Material and Methods

2.1. Maintenance of the Fungus and Culture Medium

The fungi *T. longibrachiatum* LMBC 172 used in this work were isolated from tree trunks in Ribeirão Preto, SP, Brazil. The identification and deposition with the GenBank accession code OQ255882.1 were detailed by Contato et al. [45]. Microorganism maintenance involved spore inoculation on potato dextrose agar medium (PDA) (Sigma-Aldrich, Saint Louis, MO, USA), with subsequent transfers performed in glass tubes containing the same medium. Incubation occurred at a temperature of 30 °C. Afterwards, the tubes were kept under refrigeration for up to 30 days. In addition, they were cryopreserved at -80 °C to maintain the strain for long periods of time.

2.2. Plant Material

The sugarcane bagasse originated from Pedra Agroindustrial S/A sugarcane mill (Serrana, SP, Brazil) and comprised a blend of straw, leaves, and culms from various sugarcane varieties (CTC-4, CTC-7, CTC-20, IAC95500, RB867515, and RB966928). To sanitize the material, it was immersed in 92 °GL ethanol for 1 h, followed by rinsing with

distilled water. Subsequently, the material underwent drying in an oven at 50 °C for 3 days and was then milled using a 25-mesh sieve knife mill (SL-32-SOLAB).

Tamarind (*Tamarindus indica*, Fabaceae) seeds were sourced from the campus of the University of Sao Paulo, Ribeirão Preto, SP, Brazil. The seeds underwent boiling in water for 1 h, followed by drying in an oven at 50 °C for 3 days to ensure sanitary quality and prevent the growth of other fungi. The seeds were milled using a 20-mesh sieve knife mill (SL-32-SOLAB).

2.3. Submerged Culture of *T. longibrachiatum* LMBC 172 for Protein Secretion Induction

The submerged culture procedure followed the methodology outlined by Contato et al. [45]. A spore solution containing 10^6 – 10^7 spores/mL was prepared from the fungus. The fungus was cultured in test tubes, suspended in sterile distilled water, and spore counts were conducted using a microscope and a Neubauer chamber. This suspension was then inoculated into 125 mL Erlenmeyer flasks containing 25 mL of Khanna medium (comprising Khanna's salt solution [20×]: NH_4NO_3 (2.0 g), KH_2PO_4 (1.3 g), $\text{MgSO}_4 \cdot 7\text{H}_2\text{O}$ (0.362 g), KCl (0.098 g), $\text{ZnSO}_4 \cdot \text{H}_2\text{O}$ (0.007 g), $\text{MnSO}_4 \cdot \text{H}_2\text{O}$ (0.0138 g), $\text{Fe}_2(\text{SO}_4)_3 \cdot 6\text{H}_2\text{O}$ (0.0066 g), $\text{CuSO}_4 \cdot 5\text{H}_2\text{O}$ (0.0062 g), with distilled water q.s. (100 mL) (5.0 mL); yeast extract (0.1 g); carbon source (1.0 g); distilled water q.s. to 100 mL) [48]. The media were supplemented, individually, with 1% (*w/v*) of two different lignocellulosic residues: sugarcane bagasse and tamarind seeds. Additionally, a control simulating hemicellulose was performed, individually, using a mixture containing 0.5% beechwood xylan and 0.5% oat spelt xylan (Sigma-Aldrich, Saint Louis, MO, USA). The 1% (*w/v*) ratio of lignocellulosic residues and hemicellulose simulation was chosen to evaluate the impact on CAZymes because this concentration was usually reported in studies that successfully evaluated the secretome profile of filamentous fungi [19,49,50]. After, the Erlenmeyer flasks were incubated at 30 °C under static conditions for up to 72 h, as optimal conditions for protein induction as described by Contato et al. [45].

2.4. Sample Processing

The culture supernatant of *T. longibrachiatum* cultivated in the residues under submerged conditions was harvested through filtration with Whatman filter paper Grade 1 in a vacuum pump following a 72 h period. Subsequently, it was concentrated using ultrafiltration (10,000 MWCO, PES membrane, Vivaspin, Littleton, CO, USA), then washed twice with 5 mL of 50 mM sodium acetate buffer at pH 5.0. The proteins were then subjected to separation via SDS-PAGE electrophoresis [51].

2.5. Characterization of the *T. longibrachiatum* LMBC 172 by Liquid Chromatography–Tandem Mass Spectrometry (LC–MS/MS)

For secretome LC–MS/MS analysis, 15–20 µg of total secretome proteins was loaded onto an SDS-PAGE on 12% separation gel. The gel electrophoresis employed preparative PAGE to isolate the protein secretomes from complex carbohydrate and phenolic species present in the supernatant. Electrophoresis ceased once the bromophenol blue tracking dye had migrated 2–3 cm into the separating gel. Subsequently, the gel was stained with Coomassie blue, and the entire protein banding profile was excised for processing via LC–MS/MS [52].

Isolated gel bands underwent reduction with Tris (2-carboxyethyl) phosphine, followed by alkylation using 2-iodoacetamide, and overnight digestion with 8 µg/mL trypsin in ammonium bicarbonate buffer. Peptides were extracted from the gel segments and desalted using C18 pipet tips following the manufacturer's guidelines (Agilent P/N A57003100, Agilent Technologies, Santa Clara, CA, USA). The desalted peptides were then dissolved in 0.1% aqueous formic acid and injected onto a 75-micron × 50 cm capillary HPLC column packed with 2-micron C18 particles (Thermo P/N 164942, ThermoFisher Scientific, Waltham, MA, USA) with a vented trap column setup. Peptide separation was achieved using a 60 min gradient of formic acid/acetonitrile and ionization was per-

formed in a Nanospray Flex ion source equipped with stainless-steel emitters linked to a quadrupole-Orbitrap mass spectrometer (ThermoFisher Scientific, Waltham, MA, USA).

Peptide ions were subjected to analysis using a “high-low” “top-speed” data-dependent MS/MS strategy. Precursors were initially analyzed at high resolution in the Orbitrap sector, followed by MS/MS selection in the quadrupole sector, fragmentation by HCD in the ion routing multipole, and subsequent analysis of fragment ions in the ion trap sector.

Each sample underwent LC-MS/MS analysis twice, with the two RAW data files merged into a single sample for database searching using MaxQuant (version v2.0.1.0, Max-Planck-Institute of Biochemistry, Planegg, Germany) [53]. Spectra were searched against a database containing 402,135 protein sequences obtained from the NCBI on 27 May 2022, using “*Trichoderma*” as the genus search term. Searches were annotated using Python version v3.11 (Python Software Foundation, Wilmington, DE, USA) to annotate NCBI *T. longibrachiatum* IDs by transferring annotations from related curated proteins at Uniprot (<https://www.uniprot.org/> accessed on 18 December 2022). Sequences with a false discovery rate (FDR or q-value) greater than 0.00 were removed from the analysis. Finally, we identified conserved CAZy domains using Hidden Markov Model (HMM) profiles available on the dbCAN2 web platform (<https://ccb.unl.edu/dbCAN2/index.php> accessed on 18 December 2022). Only domains with e-values $> 10^{-17}$ and coverage > 0.35 were considered.

3. Results and Discussion

Secretome Protein Composition

To elucidate the secretome of *T. longibrachiatum* LMBC 172, we gathered the culture supernatants and subjected them to LC-MS/MS analysis. Protein identifications were conducted by searching against a database of *Trichoderma* sequences obtained from the NCBI, and subsequent annotation was performed on these identified proteins. Our analyses identified 206 distinct proteins on the sum of the three different conditions (supplemented with sugarcane bagasse, or tamarind seeds, or the hemicellulose simulation) in the secretome of *T. longibrachiatum* LMBC 172 (all non-anchored extracellular proteins), of which 159 proteins were shown in the control simulating hemicellulose, 151 proteins when 1% sugarcane bagasse was used for the culture, and 118 proteins when the residue used was 1% tamarind seeds (Figure 1A). Although many proteins were coincident in the analyzed experimental conditions, there were differences in the number of proteins found, principally due to the use of beechwood xylan plus oat spelt xylan, simulating the constitution of hemicellulose, where there is a strong presence of xylan [54] (Figure 1B). The sugarcane bagasse, as demonstrated by Scarcella et al. [14], has a constitution of 159.44 ± 23.81 of xylose as the main sugar, 11-fold more than glucose (14.08 ± 4.07), the second-most abundant non-cellulosic monosaccharide. These values show the high content of hemicellulose in the structure of sugarcane bagasse. The tamarind seed is rich in xyloglucan, one of the most abundant hemicellulose polymers after xylan [44,55], thus justifying a smaller number of proteins found in the secretome when this lignocellulosic residue was used.

As can be seen in Figure 1B, of these 206 proteins found, 89 are found in all culture conditions (hemicellulose simulation, or sugarcane bagasse, or tamarind seeds). The 89 proteins found with the three different carbon sources and which biomass they degrade are shown in Table 1. Among the proteins found, there are representatives of different families such as glycosyl hydrolases (GHs) that cleave cellulose, hemicellulose, pectin, or other components; carbohydrate esterases (CEs); polysaccharide lyases (PLs); carbohydrate-binding modules (CBMs); and auxiliary activity enzymes (AAs).

Taking into analysis only the use of the hemicellulose simulation, the major proteins produced according to their iBAQ value (sum of all the peptide intensities divided by the number of observable peptides of a protein) were *endo*-1,4- β -xylanases, xylan 1,4- β -xylosidase, α -L-arabinofuranosidase, and α -galactosidase (Table 1). However, it was shown that 41 proteins were produced when only this carbon source was used (Figure 1B, Table 2). Most of these proteins are responsible for the degradation of xylan and its ramifications [56].

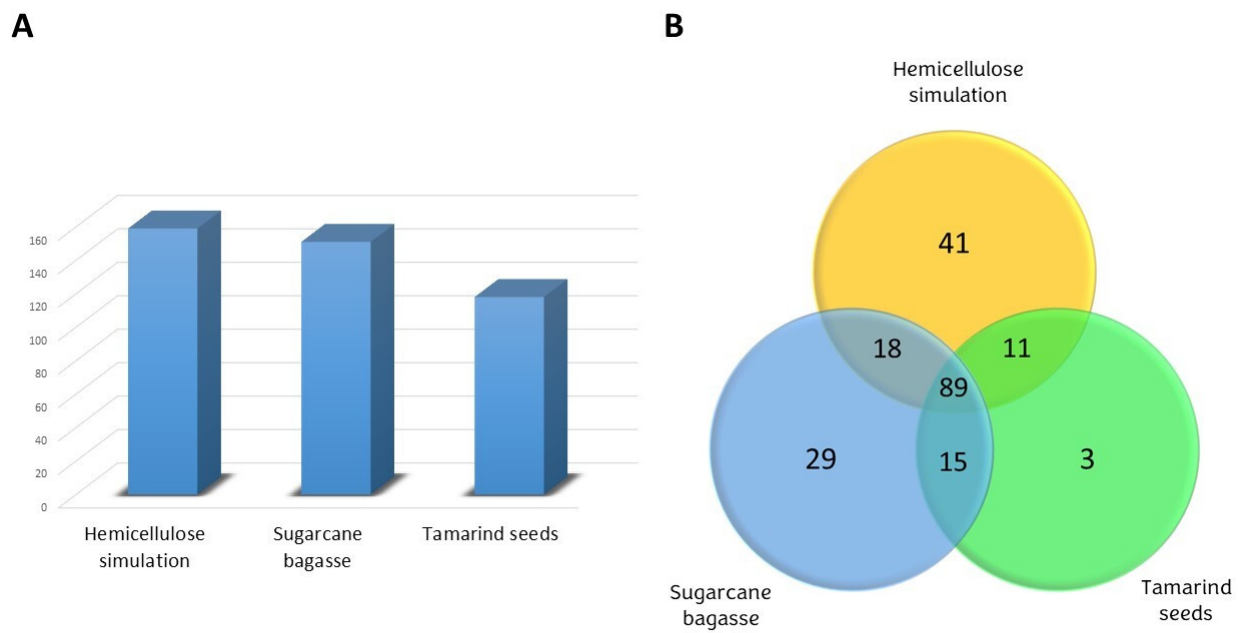


Figure 1. CAZymes from secretome analysis of *T. longibrachiatum* LMBC 172 in culture condition: hemicellulose simulation, or sugarcane bagasse, or tamarind seeds. (A) Total CAZymes found. (B) Venn plot correlating the CAZymes found in each culture condition.

Table 1. Comprehensive LC-MS/MS secretome analysis for 89 proteins found in cultures with hemicellulose simulation, sugarcane bagasse, and tamarind seeds, classified according to which substrates they degrade.

Degraded Biomass	iBAQ (a) Hemicellulose Simulation	iBAQ (a) Sugarcane Bagasse	iBAQ (a) Tamarind Seeds	Protein IDs (b)	Family	MS/MS View: Identified Proteins	Molecular Weight (kDa) (c)
amido	4.13×10^{10}	8.41×10^8	9.24×10^8	A0A2T3YUD7	GH15	glucoamylase	8
amido	1.78×10^{10}	7.88×10^8	2.24×10^8	A0A2T3ZF22	GH15	glucoamylase	33
amido	1.62×10^8	1.18×10^7	1.29×10^7	A0A2T3YUB0	GH13	α -amylase	112
carboxylic ester	1.69×10^7	6.71×10^7	1.76×10^6	A0A6V8QQW9	CE1	carboxylic ester hydrolase	36
cellulose	5.20×10^{10}	3.98×10^9	1.50×10^{10}	Q6QTF2	GH12	endoglucanase I	36
cellulose	2.32×10^{10}	5.84×10^8	7.30×10^9	A0A6V8R3W7	GH6	exoglucanase 2	64
cellulose	1.48×10^{10}	2.46×10^9	2.25×10^{10}	A0A6V8QY83	GH7	exoglucanase 1	28
cellulose	5.55×10^9	3.75×10^7	6.87×10^7	A0A6V8R5D3	GH3	β -glucosidase A	26
cellulose	3.06×10^9	3.40×10^8	4.86×10^9	A0A142C169	GH7	1,4- β -D-glucan cellobiohydrolase	33
cellulose	2.10×10^9	1.57×10^8	3.46×10^8	A0A2T3YQZ3	GH5	glycoside hydrolase	45
cellulose	1.04×10^9	7.80×10^8	8.69×10^7	KAH8124777.1	CBM35	carbohydrate-binding module	44
cellulose	4.81×10^8	2.78×10^8	1.20×10^9	A0A2T3ZAP7	CBM1	carbohydrate-binding module	88
cellulose	1.69×10^8	9.14×10^6	4.78×10^7	A0A2T3ZMC2	CBM1	carbohydrate-binding module	33
cellulose	2.96×10^7	1.90×10^8	2.20×10^8	A0A6V8R7F2	GH5	endoglucanase II	56
cellulose	2.16×10^7	4.65×10^6	7.80×10^6	A0A0W7VDH7	GH6	exoglucanase	45
cellulose	3.16×10^6	1.85×10^9	3.86×10^8	A0A6V8R5M5	GH3	β -glucosidase celA	57
chitin	2.00×10^8	1.74×10^8	3.72×10^6	XP_024756832.1	GH18	glycoside hydrolase	56

Table 1. Cont.

Degraded Biomass	iBAQ (a) Hemicellulose Simulation	iBAQ (a) Sugarcane Bagasse	iBAQ (a) Tamarind Seeds	Protein IDs (b)	Family	MS/MS View: Identified Proteins	Molecular Weight (kDa) (c)
chitin	7.88×10^7	1.66×10^7	3.31×10^5	A0A2T3YRL6	GH18	glycoside hydrolase	46
chitin	6.24×10^7	5.66×10^7	6.51×10^6	A0A2K0U0B3	GH18	chitinase	26
chitin	2.28×10^6	1.78×10^8	2.20×10^6	A0A0B5AH01	GH18	chitinase	98
cutin	1.59×10^9	2.00×10^7	2.33×10^7	A0A2T3ZC81	CE5	cutinase	42
ester carboxylic	1.05×10^8	1.65×10^8	1.42×10^8	A0A6V8R506	CE1	carboxylic ester hydrolase	55
GMC	2.17×10^7	1.33×10^8	2.46×10^7	A0A6V8R691	AA3	glucose- methanol- choline GMC oxidoreductase	57
hemicellulose	2.38×10^{11}	9.25×10^9	3.25×10^8	A0A6V8RCI3	GH3	xylan 1,4- β -xylosidase	32
hemicellulose	1.93×10^{11}	1.27×10^{10}	3.18×10^{10}	A0A6V8R417	GH54	α -L- arabinofuranosidase	85
hemicellulose	1.72×10^{11}	1.88×10^9	6.96×10^9	A0A6V8R4W9	GH11	<i>endo</i> -1,4- β - xylanase	34
hemicellulose	1.35×10^{11}	6.71×10^8	4.40×10^8	A0A6V8QYX8	GH27	α -galactosidase	57
hemicellulose	1.27×10^{11}	2.83×10^{10}	6.35×10^9	A0A088MAZ4	GH11	<i>endo</i> -1,4- β - xylanase	38
hemicellulose	3.10×10^{10}	1.02×10^8	3.73×10^9	A0A2T3YZH0	GH11	<i>endo</i> -1,4- β - xylanase	55
hemicellulose	1.27×10^{10}	4.52×10^8	4.59×10^8	A0A6V8R480	GH72	1,3- β - glucanoyltransferase	105
hemicellulose	1.03×10^{10}	1.33×10^8	1.20×10^7	G9NNL4	GH12	glycoside hydrolase	55
hemicellulose	6.63×10^9	6.27×10^8	1.97×10^8	A0A6V8QQ55	GH54	α -L- arabinofuranosidase	88
hemicellulose	5.49×10^9	2.57×10^8	3.19×10^6	A0A6V8QVE6	GH16	<i>endo</i> -1,3(4)- β - glucanase	31
hemicellulose	4.93×10^9	2.29×10^8	3.19×10^9	A0A2T3Z959	GH62	α -L- arabinofuranosidase	66
hemicellulose	4.40×10^9	3.00×10^7	1.36×10^8	A0A6V8R688	GH72	1,3- β - glucanoyltransferase	33
hemicellulose	2.17×10^9	4.19×10^6	5.16×10^5	G9N9X8	GH11	glycoside hydrolase	24
hemicellulose	1.71×10^9	1.60×10^9	1.86×10^9	A0A6V8QV79	GH43	arabinoxylan arabinofuranohy- drolase	26
hemicellulose	1.28×10^9	7.97×10^7	1.97×10^6	A0A6V8R523	GH2	β -mannosidase A	88
hemicellulose	1.24×10^9	2.84×10^7	8.89×10^7	A0A2P4ZDF2	GH27	α -galactosidase	67
hemicellulose	1.09×10^9	4.23×10^8	8.82×10^6	A0A6V8R4Z6	GH30	xylanase	52
hemicellulose	9.44×10^8	6.64×10^8	4.68×10^8	A0A6V8QNB0	GH16	glycoside hydrolase	50
hemicellulose	8.42×10^8	4.51×10^8	5.59×10^9	UKZ86534.1	GH74	xyloglucanase	78
hemicellulose	8.41×10^8	2.62×10^7	3.68×10^7	A0A6V8QP12	CE5	acetylxyylan esterase 2	53
hemicellulose	7.38×10^8	2.48×10^8	1.65×10^8	A0A6V8QM46	GH17	glucan <i>endo</i> -1,3- β -glucosidase eglC	88
hemicellulose	7.33×10^8	1.03×10^7	4.09×10^7	G9NGV2	GH27	α -galactosidase	60
hemicellulose	3.32×10^8	3.81×10^8	1.23×10^7	A0A2T3ZAU0	GH30	glycoside hydrolase	56
hemicellulose	2.74×10^8	1.65×10^8	1.44×10^6	A0A6V8R899	GH64	glucan <i>endo</i> -1,3- β -glucosidase	56
hemicellulose	2.48×10^8	2.79×10^8	9.46×10^6	A0A6V8QQA1	GH72	1,3- β - glucanoyltransferase	9
hemicellulose	1.38×10^8	5.95×10^6	3.06×10^6	A0A2N1L3Y3	CE5	acetylxyylan esterase	46

Table 1. Cont.

Degraded Biomass	iBAQ (a) Hemicellulose Simulation	iBAQ (a) Sugarcane Bagasse	iBAQ (a) Tamarind Seeds	Protein IDs (b)	Family	MS/MS View: Identified Proteins	Molecular Weight (kDa) (c)
hemicellulose	1.32×10^8	5.86×10^6	3.99×10^6	A0A0F9XN15	GH27	α -galactosidase	57
hemicellulose	1.11×10^8	3.25×10^5	3.10×10^7	A0A6V8R5J5	GH55	glucan 1,3- β -glucosidase	57
hemicellulose	1.07×10^8	5.67×10^6	5.74×10^6	A0A6V8RC59	GH27	α -galactosidase	36
hemicellulose	7.91×10^7	1.10×10^7	4.34×10^7	A0A2T4B0H5	GH54	α -L-arabinofuranosidase	102
hemicellulose	7.85×10^7	3.88×10^6	1.98×10^5	Q6QNU8	GH11	<i>endo</i> -1,4- β -xylanase	88
hemicellulose	6.42×10^7	5.76×10^8	1.14×10^8	A0A6V8QJT1	GH55	glucan 1,3- β -glucosidase	79
hemicellulose	5.74×10^7	2.15×10^7	3.48×10^6	A0A6V8QPF0	GH2	β -mannosidase A	125
hemicellulose	5.66×10^7	6.36×10^7	4.29×10^6	A0A2T3YZN9	GH78	glycoside hydrolase	40
hemicellulose	4.26×10^7	2.35×10^7	1.44×10^7	A0A2T3YYK7	GH71	glycoside hydrolase	27
hemicellulose	2.47×10^7	1.06×10^{10}	5.93×10^8	A0A6V8QIP8	GH10	<i>endo</i> -1,4- β -xylanase C	49
hemicellulose	2.12×10^7	3.21×10^7	1.65×10^6	A0A2T4C2Y0	GH72	1,3- β -glucanosyltransferase	51
hemicellulose	1.92×10^7	1.59×10^6	7.44×10^5	A0A2T4AVU1	GH17	glycoside hydrolase	88
hemicellulose	1.85×10^7	5.82×10^8	1.93×10^7	A0A2T3YYG3	GH30	glycoside hydrolase	63
hemicellulose	1.13×10^7	8.23×10^6	3.68×10^4	G0RWY3	GH18	<i>endo</i> -1,4- β -xylanase	77
hemicellulose	8.92×10^6	6.19×10^8	3.87×10^7	A0A6V8R5H6	GH35	β -galactosidase	60
hemicellulose	8.60×10^6	1.64×10^6	1.88×10^5	A0A2T3Z3S2	GH27	α -galactosidase	87
hemicellulose	3.74×10^6	2.33×10^8	2.02×10^6	A0A2T3ZG69	GH31	glycoside hydrolase	89
hemicellulose	3.40×10^6	6.90×10^9	2.42×10^8	XP_024755433.1	GH10	glycoside hydrolase	57
hemicellulose	1.49×10^6	3.32×10^7	2.49×10^7	A0A6V8R3D3	GH3	xylan 1,4- β -xylosidase	65
hemicellulose	1.39×10^6	1.87×10^8	2.57×10^6	A0A6V8QXM8	GH67	α -glucuronidase	55
hemicellulose	6.91×10^5	1.42×10^7	4.53×10^6	A0A6V8QX14	GH76	mannan <i>endo</i> -1,6- α -mannosidase	44
hemicellulose	6.50×10^5	8.42×10^6	2.19×10^5	A0A2T3YZP2	GH79	glycoside hydrolase	97
lignin	1.69×10^9	1.44×10^9	1.83×10^6	A0A6V8QZK1	AA3	laccase	70
oxygen	1.25×10^8	4.76×10^7	8.71×10^5	A0A6V8R4F9	AA3	FAD-dependent monooxygenase	54
pectin	1.26×10^{11}	6.11×10^9	1.58×10^9	A0A2T3YXQ4	CE5	carbohydrate esterase	56
pectin	3.20×10^{10}	3.13×10^7	1.34×10^9	A0A6V8R602	GH28	endopolygalacturonase	56
pectin	1.52×10^{10}	1.12×10^9	2.57×10^8	XP_024766320.1	CE5	carbohydrate esterase	49
pectin	5.45×10^9	4.68×10^8	6.53×10^8	A0A2K0T4R7	CE5	cutinase	48
pectin	3.53×10^9	1.35×10^6	1.05×10^7	A0A6V8QQH8	PL7	alginate lyase	88
pectin	2.31×10^9	1.04×10^7	3.93×10^7	A0A6V8R557	PL1	polysaccharide lyase	42
pectin	1.53×10^9	4.76×10^7	5.34×10^8	A0A2T3YYD8	CE8	pectinesterase	36
pectin	5.65×10^8	4.01×10^8	4.44×10^7	A0A2T3YTH0	GH28	glycoside hydrolase	65
pectin	2.87×10^8	4.01×10^5	1.85×10^8	A0A2T3YUA1	GH28	glycoside hydrolase	34
pectin	1.79×10^8	1.61×10^7	7.61×10^6	A0A2T3ZG56	GH28	glycoside hydrolase	56

Table 1. Cont.

Degraded Biomass	iBAQ (a) Hemicellulose Simulation	iBAQ (a) Sugarcane Bagasse	iBAQ (a) Tamarind Seeds	Protein IDs (b)	Family	MS/MS View: Identified Proteins	Molecular Weight (kDa) (c)
pectin	1.13×10^8	3.68×10^7	1.33×10^8	A0A395NND2	GH28	glycoside hydrolase	50
pectin	8.22×10^7	6.60×10^7	1.40×10^7	A0A2T3ZCA4	CE16	carbohydrate esterase	26
pectin	1.94×10^7	3.74×10^5	1.17×10^5	A0A2T3YZM0	GH18	glycoside hydrolase	39
pectin	2.24×10^6	1.43×10^6	9.20×10^7	A0A6V8RBF6	PL1	pectate lyase C	68
pectin	1.61×10^5	5.72×10^6	5.28×10^6	A0A2T3YUJ2	GH28	glycoside hydrolase	71
phosphate	3.60×10^8	6.77×10^7	6.38×10^5	A0A6V8QHF9	CBM21	acid phosphatase	44

(a) The iBAQ corresponds to the sum of all the peptide intensities divided by the number of observable peptides of a protein. (b) Accession number with protein information and family information were obtained from UniProt/Swiss-Prot database or NCBI database. (c) Hypothetical molecular weight of the proteins.

Table 2. Comprehensive LC-MS/MS secretome analysis for 41 proteins found only in the hemicellulose simulation conditions classified according to which biomass they degrade.

Degraded Biomass	iBAQ (a) Hemicellulose Simulation	Protein IDs (b)	Family	MS/MS View: Identified Proteins	Molecular Weight (kDa) (c)
amido	6.46×10^7	A0A2T4B8C2	CE50	amidase	49
cellulose	1.05×10^8	A0A2T3Z508	CBM1	carbohydrate- binding module	28
cellulose	4.09×10^7	G9P6M2	CE5	carbohydrate esterase	53
cellulose	3.37×10^7	A0A2K0SW07	CBM1	carbohydrate- binding module	78
cellulose	2.07×10^7	A0A2T3YUC4	GH3	β -glucosidase	55
cellulose	1.41×10^7	A0A2T3YX19	CBM1	carbohydrate- binding module	52
cellulose	1.37×10^7	A0A2T4BD17	CBM1	carbohydrate- binding module	42
cellulose	1.09×10^7	A0A2T3Z5Y5	CBM18	carbohydrate- binding module	55
cellulose	9.31×10^6	A0A6V8R0S9	AA9	lytic polysaccharide monooxygenase	40
cellulose	3.65×10^6	G9NFW5	GH5	glycoside hydrolase	50
cellulose	2.95×10^6	A0A395NHN7	GH7	cellobiohydrolase	25
cellulose	2.28×10^6	A0A2K0TAX7	AA9	copper radical oxidase	43
cellulose	1.96×10^6	G9N4X9	GH5	glycoside hydrolase	115
chitin	2.27×10^8	A0A6V8R2F4	GH18	chitinase	44
chitin	7.82×10^6	A0A2K0T4Z2	GH18	chitinase	49
hemicellulose	3.57×10^8	A0A6V8QJU6	CE6	acetylxylan esterase	46
hemicellulose	8.52×10^7	A0A2H2ZRV5	CE5	acetylxylan esterase	36
hemicellulose	7.56×10^7	A0A0W7VKU2	GH54	α -L- arabinofuranosidase	102
hemicellulose	6.34×10^7	G9N626	GH27	α -galactosidase	32
hemicellulose	4.66×10^7	A0A395NVC4	GH3	xylan 1,4- β -xylosidase	58
hemicellulose	4.39×10^7	A0A6V8QTS4	GH16	glucan <i>endo</i> -1,3- β - glucosidase	44

Table 2. Cont.

Degraded Biomass	iBAQ (a) Hemicellulose Simulation	Protein IDs (b)	Family	MS/MS View: Identified Proteins	Molecular Weight (kDa) (c)
hemicellulose	3.29×10^7	A0A6V8QPH8	GH76	mannan <i>endo</i> -1,6- α -mannosidase	34
hemicellulose	3.03×10^7	KAH6604482.1	GH11	glycoside hydrolase	56
hemicellulose	3.01×10^7	A0A2K0TP30	GH16	glycoside hydrolase	49
hemicellulose	2.69×10^7	G9NUB8	GH62	α -L-arabinofuranosidase	51
hemicellulose	2.44×10^7	A0A2T3YUG9	GH3	xylan 1,4- β -xylosidase	25
hemicellulose	1.82×10^7	A0A2T4ASM6	GH3	xylan 1,4- β -xylosidase	31
hemicellulose	1.54×10^7	G9MSH9	GH3	xylan 1,4- β -xylosidase	15
hemicellulose	1.40×10^7	A0A2T3YT55	GH54	α -L-arabinofuranosidase	40
hemicellulose	1.24×10^7	A0A395NS24	GH54	α -L-arabinofuranosidase	27
hemicellulose	9.94×10^6	A0A2T4BTG8	GH54	α -L-arabinofuranosidase	46
hemicellulose	7.48×10^6	G9MZ65	GH54	α -L-arabinofuranosidase	28
hemicellulose	6.24×10^6	G9MV41	GH27	α -galactosidase	69
hemicellulose	5.24×10^6	A0A6V8R9B0	GH27	α -galactosidase	42
hemicellulose	4.48×10^6	A0A2K0UKQ2	GH3	xylan 1,4- β -xylosidase	26
hemicellulose	3.55×10^6	G9P179	GH3	xylan 1,4- β -xylosidase	55
hemicellulose	2.72×10^6	A0A395NKK0	GH12	glycoside hydrolase	120
hemicellulose	1.11×10^6	G9NPZ0	GH64	glycoside hydrolase	45
pectin	1.20×10^8	G9NBD3	CE5	carbohydrate esterase	65
pectin	4.64×10^7	G9NXF6	CE5	carbohydrate esterase	52
pectin	1.60×10^6	G9NPZ7	CE5	carbohydrate esterase	49

(a) The iBAQ corresponds to the sum of all the peptide intensities divided by the number of observable peptides of a protein. (b) Accession number with protein information and family information were obtained from UniProt/Swiss-Prot database or NCBI database. (c) Hypothetical molecular weight of the proteins.

On the other hand, it was shown that *T. longibrachiatum* LMBC 172 secreted 29 unique proteins with the use of sugarcane bagasse as the carbon source (Figure 1B, Table 3), with emphasis on 2 glycosyl hydrolases of the GH92 family, a family recognized to belong to α -mannosidases [57], in addition to 2 more mannan *endo*-1,6- α -mannosidases from the GH76 family, in agreement with the study by Scarcella et al. [14], who showed a mannose composition in sugarcane bagasse. Another enzyme found that agrees with the study by Scarcella et al. [14] is the α -fucosidase A of the GH95 family, given the existence of fucose in the constitution of this residue. Another interesting finding when using sugarcane bagasse for the culture was the great iBAQ shown in the production of a glycosyl hydrolase from the GH93 family: the GH93 family hydrolyses linear α -1,5-L-arabinan [58].

Table 3. Comprehensive LC-MS/MS secretome analysis for 29 proteins enzymes found only in the sugarcane bagasse culture classified according to which biomass they degrade.

Degraded Biomass	iBAQ (a) Sugarcane Bagasse	Protein IDs (b)	Family	MS/MS View: Identified Proteins	Molecular Weight (kDa) (c)
amido	4.51×10^6	B5BQC3	GH13	α -amylase	57
carboxylic ester	1.37×10^8	A0A6V8QU70	CE1	carboxylic ester hydrolase	56
carboxylic ester	3.42×10^7	A0A2T3ZJ05	CE1	carboxylic ester hydrolase	26
carboxylic ester	1.03×10^7	A0A6V8R5C2	CE1	carboxylic ester hydrolase	70
carboxylic ester	8.95×10^6	A0A2K0U229	CE1	carboxylic ester hydrolase	60
cellulose	9.08×10^7	A0A6V8QJS6	GH3	β -glucosidase F	46
cellulose	3.84×10^7	A0A395N8R8	GH2	glycoside hydrolase	25
cellulose	1.99×10^7	A0A6V8QPG8	GH31	α -glucosidase	31
cellulose	9.93×10^6	G9P291	GH3	glycoside hydrolase	25
cellulose	4.39×10^6	A0A2T4CHF3	GH3	β -glucosidase	96
cellulose	2.32×10^6	A0A2T3YT78	GH3	β -glucosidase	28
chitin	2.29×10^7	V9I0I2	GH18	chitinase	42
chitin	4.68×10^6	A0A395NWN8	GH75	<i>endo</i> -chitinase	88
fucose	1.33×10^7	A0A6V8QZS6	GH95	α -fucosidase A	26
hemicellulose	2.46×10^8	A0A2T3ZFW9	GH92	glycoside hydrolase	88
hemicellulose	9.26×10^7	A0A6V8QLJ6	GH76	mannan <i>endo</i> -1,6- α - mannosidase	25
hemicellulose	3.34×10^7	A0A6V8QYK7	GH43	arabinoxylan arabino- furanohydrolase	56
hemicellulose	3.21×10^7	A0A2T3ZL91	GH16	glycoside hydrolase	72
hemicellulose	1.86×10^7	A0A6V8R1B3	GH51	α -L- arabinofuranosidase	36
hemicellulose	9.40×10^6	A0A0F9XAZ2	GH43	glycoside hydrolase	47
hemicellulose	5.84×10^6	A0A6V8R596	GH5	glucan <i>endo</i> -1,6- β - glucosidase B	26
hemicellulose	4.36×10^6	A0A2T3YUM4	GH55	glycoside hydrolase	80
hemicellulose	4.34×10^6	A0A2P4ZLF1	GH6	α -galactosidase	27
hemicellulose	2.56×10^6	A0A395NYK8	GH71	glycoside hydrolase	42
hemicellulose	2.42×10^6	A0A1T3CS19	GH76	mannan <i>endo</i> -1,6- α - mannosidase	58
hemicellulose	2.13×10^6	G9PBD3	GH72	1,3- β - glucanosyltransferase	49
hemicellulose	1.74×10^6	G9NFR0	GH93	glycoside hydrolase	49
hemicellulose	1.67×10^6	A0A2T3YT16	GH17	glycoside hydrolase	23
hemicellulose	1.49×10^6	A0A2T3YQY4	GH92	glycoside hydrolase	25

(a) The iBAQ corresponds to the sum of all the peptide intensities divided by the number of observable peptides of a protein. (b) Accession number with protein information and family information were obtained from UniProt/Swiss-Prot database or NCBI database. (c) Hypothetical molecular weight of the proteins.

A different analysis was shown when tamarind seeds were used for the culture, since only three proteins were produced exclusively with the use of this lignocellulosic residue (Figure 1B), which were a carbohydrate-binding module CBM1, a glycosyl hydrolase of the GH5 family, and curiously a laccase, an enzyme recognized for being a polyphenol oxidase [59] (Table 4). However, an interesting verification is the fact of the great iBAQ shown in the production of a xyloglucanase of the GH74 family when using tamarind

seeds in comparison with the other conditions (Table 1), thus reaffirming the richness of xyloglucan in the constitution of these seeds.

Table 4. Comprehensive LC-MS/MS secretome analysis for three proteins found only in the tamarind seeds condition classified according to which biomass they degrade.

Degraded Biomass	iBAQ (a) Tamarind Seeds	Protein IDs (b)	Family	MS/MS View: Identified Proteins	Molecular Weight (kDa) (c)
cellulose	3.03×10^8	G9PBZ8	GH5	glycoside hydrolase	88
cellulose	3.01×10^6	A0A2T3YZD8	CBM1	carbohydrate- binding module	34
lignin	1.07×10^8	A0A2T3YR43	AA3	laccase	45

(a) The iBAQ corresponds to the sum of all the peptide intensities divided by the number of observable peptides of a protein. (b) Accession number with protein information and family information were obtained from UniProt/Swiss-Prot database or NCBI database. (c) Hypothetical molecular weight of the proteins.

Other important data to be analyzed are the proteins found in only two of the three conditions tested and the reasons for this. When using the simulation of hemicellulose and sugarcane bagasse for the culture, 18 proteins in common are shown, which are not found when the culture was made with tamarind seeds (Figure 1B). Among the most interesting are a lysozyme of the GH25 family, which promotes the hydrolysis of the β -1,4 glycosidic bonds between residues of *N*-acetylmuramic acid (Mur2Ac) and *N*-acetyl-D-glucosamine (GlcNAc) in a peptidoglycan [60]; and a β -glucuronidase of the GH79 family (Table S1—Supplementary Material). However, the great majority of these 18 proteins are enzymes that cleave xylan, a polysaccharide seen in smaller amounts in tamarind seeds.

The correlation of the CAZymes shown in the secretome of *T. longibrachiatum* LMBC 172 when cultivated with the hemicellulose simulation or with tamarind seeds was performed, and it was seen that 11 proteins are found (Figure 1B); specifically, α -L-arabinofuranosidases belonging to the GH54 family were investigated. These enzymes are responsible for hydrolyzing terminal α -1,5-glycosidic linkages to arabinofuranosides in arabinan, as well as α -1,2 and α -1,3-linkages to arabinofuranosides of arabinan, arabinoxylan, and arabinogalactan. They operate synergistically with other hemicellulolytic enzymes, effectively removing L-arabinose side chains that might otherwise impede the activity of backbone-degrading enzymes [61]. Other proteins found are the glycosyl hydrolases of the GH7 family that cleave β -1,4 glycosidic bonds in cellulose/ β -1,4-glucans [62] (Table S2—Supplementary Material). It is agreement the presence, simultaneous between these conditions (hemicellulose simulation and tamarind seeds), of enzymes that cleave cellulose existing in the medium.

Analyzing the CAZymes shown simultaneously among the cultures performed with lignocellulosic residues, sugarcane bagasse, or tamarind seeds, 15 proteins are found in common (Figure 1B), especially a feruloyl esterase C, a mannosyl-oligosaccharide α -1,2-mannosidase of the GH47 family, an AA9 lytic polysaccharide monoxygenase, and a glycosyl hydrolase from the GH39 family, recognized to belong to β -xylosidase [63] (Table S3—Supplementary Material). However, the great majority are CAZymes from the GH3 family, which currently groups together *exo*-acting β -D-glucosidases, α -L-arabinofuranosidases, and β -D-xylopyranosidases [64], enzymes known to be hemicelluloses.

The secreted enzymes of *T. longibrachiatum* differ when using sugarcane bagasse, or tamarind seeds, or hemicellulose simulation due to the distinct composition of the polysaccharides present in these carbon sources. Sugarcane bagasse primarily consists of cellulose, hemicellulose, and lignin, with cellulose being the most abundant polysaccharide [36–38]. As a result, the secretome of *T. longibrachiatum* grown on sugarcane bagasse is rich in cellulases, such as GH3, GH5, GH6, and GH7, which are crucial for breaking down cellulose into glucose monomers (Tables 1 and 3). Additionally, the presence of hemicellulose and lignin in sugarcane bagasse stimulates the production of hemicellulases (e.g., xylanases, GH10) and lignin-degrading auxiliary activity enzymes (AAs) like AA3 and AA9 (Table 1

and Table S3—Supplementary Material), facilitating the comprehensive degradation of this complex biomass.

In contrast, tamarind seeds contain high levels of xyloglucans, which are polysaccharides composed of a cellulose backbone with xylose, galactose, and fucose side chains [43,44]. The unique structure of xyloglucans in tamarind seeds necessitates the production of specific enzymes, such as xyloglucanases (GH74), to effectively hydrolyze these complex sugars [19]. Consequently, the secretome of *T. longibrachiatum* cultured with tamarind seeds is particularly enriched in enzymes that target xyloglucans (Table 1), reflecting the adaptation of the fungus to the predominant polysaccharides in this carbon source.

Hemicellulose simulation, which likely includes a mixture of various hemicellulosic sugars such as xylans, mannans, and arabinogalactans, prompts the secretion of a diverse array of hemicellulases tailored to these components. Enzymes such as xylanases (GH11), mannosidases (GH76), and arabinofuranosidases (GH54) are produced to degrade the heterogeneous polysaccharide structure of hemicellulose into fermentable sugars (Tables 1 and 2; and Tables S1 and S2—Supplementary Material) [46,47].

The differences in secreted enzymes when using sugarcane bagasse, or tamarind seeds, or hemicellulose are thus directly influenced by the specific polysaccharide compositions of these substrates. The fungus adapts its enzymatic machinery to efficiently break down the available sugars, producing a tailored set of CAZymes that correspond to the structural complexity and specificities of the given carbon source. This adaptive enzyme production ensures the optimal utilization of the provided biomass, demonstrating the metabolic versatility of *T. longibrachiatum*.

These results demonstrate the importance of analysis studies of CAZymes secreted by microorganisms in different culture conditions, since their abundance in relation to protein intensity can present different results [65]. In addition, they agree with previous works published by our group, such as that of Contato et al. [45], which provides, under the same culture conditions, the catalytic activity of the enzymes found in the *T. longibrachiatum* LMBC 172 secretome shown in this study. The research identified a total of 206 distinct CAZymes in the secretome of *T. longibrachiatum* LMBC 172, with 89 proteins consistently produced across all three conditions (sugarcane bagasse, or tamarind seeds, or hemicellulose simulation). Notably, specific proteins were uniquely produced depending on the carbon source, including 41 proteins for hemicellulose simulation, 29 for sugarcane bagasse, and 3 for tamarind seeds. Tamarind seeds, specifically, induced a high production of xyloglucanase GH74, reflecting their high xyloglucan content [44].

The identified CAZymes belong to various families, such as glycosyl hydrolases (GHs), carbohydrate esterases (CEs), polysaccharide lyases (PLs), carbohydrate-binding modules (CBMs), and auxiliary activity enzymes (AAs). The study underscores the adaptive mechanisms of *T. longibrachiatum* in secreting differential enzymes based on the carbon source, which is crucial for the degradation of specific components of lignocellulosic biomass. This differential enzyme secretion highlights the fungus's ability to utilize diverse carbon sources effectively [23,24,26,29,66,67].

From a biotechnological perspective, the detailed secretome analysis of *T. longibrachiatum* can drive the development of efficient enzyme cocktails for biomass conversion processes, thereby enhancing the production of biofuels and biochemicals [24,68,69]. The specific enzymes identified in this study hold potential for further engineering or optimization for various industrial applications, including the food, beverage, textile, and paper industries [25,68,70,71]. Additionally, utilizing agricultural residues like sugarcane bagasse and tamarind seeds as carbon sources for enzyme production promotes sustainable biomass utilization, reducing environmental waste and supporting circular bioeconomy initiatives [14,26,45,72]. The ability of *T. longibrachiatum* to produce different enzymes tailored to specific substrates suggests potential for customized enzyme production to meet specific industrial needs.

Environmentally, this study supports efforts to mitigate the impact of waste disposal by leveraging agro-industrial residues, thus promoting the efficient use of renewable resources.

The findings advocate for eco-friendly alternatives to traditional chemical processing methods, reducing reliance on non-renewable resources and minimizing environmental pollution. Furthermore, this research advances the understanding of molecular mechanisms behind enzyme production and secretion in fungi, contributing significantly to the field of fungal biotechnology. Insights gained from this study can inform future research on other fungal species and their potential applications in various biotechnological processes.

In summary, this study provides a comprehensive analysis of the CAZyme secretome of *T. longibrachiatum* under different conditions, highlighting significant biotechnological advancements and sustainable industrial applications. The research emphasizes the potential for developing efficient and tailored enzyme solutions to meet the growing demand for sustainable biomass conversion and industrial bioprocessing.

4. Conclusions

The analysis of the secretome of *T. longibrachiatum* LMBC 172 cultured under submerged fermentation in two different lignocellulosic residues, sugarcane bagasse or tamarind seeds, in addition to a hemicellulose simulation as the control, revealed a total of 206 CAZymes. Each carbon source showed particularities and differences. Of these, 89 proteins were produced simultaneously with all the carbon sources, 41 proteins using only the hemicellulose simulation, 29 proteins when sugarcane bagasse was used as a carbon source, and only 3 when tamarind seeds were used. Among the proteins found, there are representatives of different families such as glycosyl hydrolases (GHs) that cleave cellulose, hemicellulose, pectin, or other components; carbohydrate esterases (CEs); polysaccharide lyases (PLs); carbohydrate-binding modules (CBMs); and auxiliary activity enzymes (AAs). These results demonstrate the importance of analysis studies of CAZymes secreted by microorganisms in different culture conditions, since their abundance in relation to protein intensity can present different results. However, it has limitations that need addressing. The secretome analysis, though detailed, was based on a limited number of carbon sources, and expanding the range of substrates could provide a broader understanding of the enzyme production capabilities of *T. longibrachiatum*. Future research should explore the genetic and metabolic pathways involved in enzyme regulation and secretion, as well as investigate the synergistic effects of mixed carbon sources on enzyme profiles.

Supplementary Materials: The following supporting information can be downloaded at: <https://www.mdpi.com/article/10.3390/cleantechnol6030050/s1>, Table S1: Comprehensive LC-MS/MS secretome analysis for 18 proteins found using the simulation of hemicellulose and sugarcane bagasse classified according to which biomass they degrade; Table S2: Comprehensive LC-MS/MS secretome analysis for 11 proteins found using the simulation of hemicellulose and tamarind seeds classified according to which biomass they degrade; Table S3: Comprehensive LC-MS/MS secretome analysis for 15 proteins found using sugarcane bagasse and tamarind seeds classified according to which biomass they degrade.

Author Contributions: A.G.C.: methodology, investigation, data curation, formal analysis, writing—original draft. T.C.B.: methodology, investigation, data curation, formal analysis. A.K.F.d.C.: writing—review and editing. H.B.S.B.: writing—review and editing. M.S.B.: funding acquisition, conceptualization. J.R.: methodology, investigation, data curation, formal analysis, writing—review and editing. S.H.: methodology, investigation, data curation, formal analysis, writing—review and editing. R.A.P.: methodology, investigation, data curation, formal analysis, funding acquisition, supervision, writing—review and editing. M.d.L.T.d.M.P.: funding acquisition, conceptualization, supervision, writing—review and editing. All authors have read and agreed to the published version of the manuscript.

Funding: The authors thank the Fundação de Amparo à Pesquisa do Estado de São Paulo (FAPESP) for the doctorate grants awarded to A.G. Contato (Processes n° 2017/25862-6 and 2021/07066-3), and to T.C. Borelli (Process n° 2021/08235-3); and financial support from the National Institute of Science and Technology of Bioethanol (Process FAPESP 2014/50884-5), and Process FAPESP 2018/07522-6. Conselho Nacional de Desenvolvimento Científico (CNPq), processes 465319/2014-9. M.L.T.M. Polizeli (process 310340/2021-7) and M.S. Buckeridge are Research Fellows of CNPq.

Institutional Review Board Statement: The study adheres to all ethical guidelines, including compliance with the legal regulations of the countries where the research was conducted.

Informed Consent Statement: Not applicable.

Data Availability Statement: The datasets produced and analyzed during this study are accessible upon reasonable request from the corresponding author.

Acknowledgments: Mass spectrometry analyses and primary database searches were performed at the Center for Genomics and Proteomics, situated at Oklahoma State University.

Conflicts of Interest: The authors assert that there are no apparent competing financial interests or personal relationships that might have influenced the findings presented in this paper.

References

1. Ravindra, K.; Singh, T.; Mor, S. Emissions of air pollutants from primary crop residue burning in India and their mitigation strategies for cleaner emissions. *J. Clean. Prod.* **2019**, *208*, 261–273. [[CrossRef](#)]
2. Yadav, M.; Paritosh, K.; Pareek, N.; Vivekanand, V. Coupled treatment of lignocellulosic agricultural residues for augmented biomethanation. *J. Clean. Prod.* **2019**, *213*, 75–88. [[CrossRef](#)]
3. Singh, T.A.; Sharma, M.; Sharma, M.; Sharma, G.D.; Passari, A.K.; Bhasin, S. Valorization of agro-industrial residues for production of commercial biorefinery products. *Fuel* **2022**, *322*, 124284. [[CrossRef](#)]
4. Pasin, T.M.; Almeida, P.Z.; Scarcella, A.S.A.; Infante, J.; Polizeli, M.L.T.M. Bioconversion of agro-industrial residues to second-generation bioethanol. In *Biorefinery of Alternative Resources: Targeting Green Fuels and Platform Chemicals*; Nanda, S., Vo, D.V.N., Sarangi, P.K., Eds.; Springer Nature: Berlin, Germany, 2020; pp. 23–47.
5. Bechara, R.; Gomez, A.; Saint-Antonin, J.M.; Schweitzer, J.M.; Maréchal, F.; Ensinas, A. Review of design works for the conversion of sugarcane to first and second-generation ethanol and electricity. *Renew. Sustain. Energy Rev.* **2018**, *91*, 152–164. [[CrossRef](#)]
6. Klein, B.C.; Sampaio, I.L.M.; Mantelatto, P.E.; Filho, R.M.; Bonomi, A. Beyond ethanol, sugar, and electricity: A critical review of product diversification in Brazilian sugarcane mills. *Biofuel Bioprod. Biorefin.* **2019**, *13*, 809–821. [[CrossRef](#)]
7. Pereira, L.G.; Cavalett, O.; Bonomi, A.; Zhang, Y.; Warner, E.; Chum, H.L. Comparison of biofuel life-cycle GHG emissions assessment tools: The case studies of ethanol produced from sugarcane, corn, and wheat. *Renew. Sustain. Energy Rev.* **2019**, *110*, 1–12. [[CrossRef](#)]
8. Yamaguchi, A.; Mimura, N.; Shirai, M.; Sato, O. Cascade utilization of biomass: Strategy for conversion of cellulose, hemicellulose, and lignin into useful chemicals. *ACS Sustain. Chem. Eng.* **2019**, *7*, 10445–10451. [[CrossRef](#)]
9. Vaidya, A.A.; Murton, K.D.; Smith, D.A.; Dedual, G. A review on organosolv pretreatment of softwood with a focus on enzymatic hydrolysis of cellulose. *Biomass Convers. Biorefin.* **2022**, *12*, 5427–5442. [[CrossRef](#)]
10. Loqué, D.; Scheller, H.V.; Pauly, M. Engineering of plant cell walls for enhanced biofuel production. *Curr. Opin. Plant Biol.* **2015**, *25*, 151–161. [[CrossRef](#)]
11. Martínez-Sanz, M.; Lopez-Sanchez, P.; Gidley, M.J.; Gilbert, E.P. Evidence for differential interaction mechanism of plant cell wall matrix polysaccharides in hierarchically-structured bacterial cellulose. *Cellulose* **2015**, *22*, 1541–1563. [[CrossRef](#)]
12. Binod, P.; Gnansounou, E.; Sindhu, R.; Pandey, A. Enzymes for second generation biofuels: Recent developments and future perspectives. *Bioresour. Technol. Rep.* **2019**, *5*, 317–325. [[CrossRef](#)]
13. Brück, S.A.; Contato, A.G.; Gamboa-Trujillo, P.; de Oliveira, T.B.; Cereia, M.; Polizeli, M.L.T.M. Prospection of psychrotrophic filamentous fungi isolated from the High Andean Paramo region of northern Ecuador: Enzymatic activity and molecular identification. *Microorganisms* **2022**, *10*, 282. [[CrossRef](#)] [[PubMed](#)]
14. Scarcella, A.S.A.; Pasin, T.M.; de Lucas, R.C.; Ferreira-Nozawa, M.S.; de Oliveira, T.B.; Contato, A.G.; Grandis, A.; Buckeridge, M.S.; Polizeli, M.L.T.M. Holocellulase production by filamentous fungi: Potential in the hydrolysis of energy cane and other sugarcane varieties. *Biomass Convers. Biorefin.* **2023**, *13*, 1163–1174. [[CrossRef](#)]
15. Behera, S.S.; Ray, R.C. Solid state fermentation for production of microbial cellulases: Recent advances and improvement strategies. *Int. J. Biol. Macromol.* **2016**, *86*, 656–669. [[CrossRef](#)] [[PubMed](#)]
16. Pellegrin, C.; Morin, E.; Martin, F.M.; Veneault-Fourrey, C. Comparative analysis of secretomes from ectomycorrhizal fungi with an emphasis on small-secreted proteins. *Front. Microbiol.* **2015**, *6*, 1278. [[CrossRef](#)] [[PubMed](#)]
17. Basotra, N.; Kaur, B.; Di Falco, M.; Tsang, A.; Chadha, B.S. *Mycothermus thermophilus* (Syn. *Scytalidium thermophilum*): Repertoire of a diverse array of efficient cellulases and hemicellulases in the secretome revealed. *Bioresour. Technol.* **2016**, *222*, 413–421. [[CrossRef](#)] [[PubMed](#)]
18. Raheja, Y.; Kaur, B.; Falco, M.; Tsang, A.; Chadha, B.S. Secretome analysis of *Talaromyces emersonii* reveals distinct CAZymes profile and enhanced cellulase production through response surface methodology. *Ind. Crops Prod.* **2020**, *152*, 112554. [[CrossRef](#)]
19. Contato, A.G.; Borelli, T.C.; Buckeridge, M.S.; Rogers, J.; Hartson, S.; Prade, R.A.; Polizeli, M.L.T.M. Secretome analysis of *Thermothelomyces thermophilus* LMBC 162 cultivated with *Tamarindus indica* seeds reveals CAZymes for degradation of lignocellulosic biomass. *J. Fungi* **2024**, *10*, 121. [[CrossRef](#)] [[PubMed](#)]
20. Barrett, K.; Jensen, K.; Meyer, A.S.; Frisvad, J.C.; Lange, L. Fungal secretome profile categorization of CAZymes by function and family corresponds to fungal phylogeny and taxonomy: Example *Aspergillus* and *Penicillium*. *Sci. Rep.* **2020**, *10*, 5158. [[CrossRef](#)]

21. Filiatrault-Chastel, C.; Heiss-Blanquet, S.; Margeot, A.; Berrin, J.G. From fungal secretomes to enzymes cocktails: The path forward to bioeconomy. *Biotechnol. Adv.* **2021**, *52*, 107833. [CrossRef]
22. Samuels, G.J.; Ismaiel, A.; Mulaw, T.B.; Szakacs, G.; Druzhinina, L.S.; Kubicek, C.P.; Jaklitsch, W.M. The Longibrachiatum Clade of *Trichoderma*: A revision with new species. *Fungal Divers.* **2012**, *55*, 77–108. [CrossRef] [PubMed]
23. Li, W.; Zhao, L.; He, X. Degradation potential of different lignocellulosic residues by *Trichoderma longibrachiatum* and *Trichoderma afroharzianum* under solid state fermentation. *Process Biochem.* **2022**, *112*, 6–17. [CrossRef]
24. Contato, A.G.; Nogueira, K.M.V.; Buckeridge, M.S.; Silva, R.N.; Polizeli, M.L.T.M. *Trichoderma longibrachiatum* and *Thermothelomyces thermophilus* co-culture: Improvement the saccharification profile of different sugarcane bagasse varieties. *Biotechnol. Lett.* **2023**, *45*, 1093–1102. [CrossRef] [PubMed]
25. Kunamneni, A.; Plou, F.J.; Alcalde, M.; Ballesteros, A. *Trichoderma* enzymes for food industries. In *Biotechnology and Biology of Trichoderma*; Elsevier: Amsterdam, The Netherlands, 2014; pp. 339–344.
26. Contato, A.G.; Vici, A.C.; Pinheiro, V.E.; de Oliveira, T.B.; de Freitas, E.N.; Aranha, G.M.; Junior, A.L.A.V.; Vargas-Rechia, C.G.; Buckeridge, M.S.; Polizeli, M.L.T.M. Comparison of *Trichoderma longibrachiatum* xyloglucanase production using tamarind (*Tamarindus indica*) and jatoba (*Hymenaea courbaril*) seeds: Factorial design and immobilization on ionic supports. *Fermentation* **2022**, *8*, 510. [CrossRef]
27. Camacho-Luna, V.; Pizar-Quiroz, A.M.; Rodríguez-Hernández, A.A.; Rodríguez-Monroy, M.; Sepúlveda-Jiménez, G. *Trichoderma longibrachiatum*, a biological control agent of *Sclerotium cepivorum* on onion plants under salt stress. *Biol. Control* **2023**, *180*, 105168. [CrossRef]
28. Degani, O.; Rabinovitz, O.; Becher, P.; Gordani, A.; Chen, A. *Trichoderma longibrachiatum* and *Trichoderma asperellum* confer growth promotion and protection against late wilt disease in the field. *J. Fungi* **2021**, *7*, 444. [CrossRef] [PubMed]
29. Pachauri, P.V.A.; More, S.; Sullia, S.B.; Deshmukh, S. Purification and characterization of cellulase from a novel isolate of *Trichoderma longibrachiatum*. *Biofuels* **2020**, *11*, 85–91. [CrossRef]
30. Ashfaque, M.; Solomon, S.; Pathak, N. Kinetic study of immobilized cellobiase produced from immobilized wild-type *Trichoderma longibrachiatum*. *Sugar Tech* **2016**, *18*, 340–346. [CrossRef]
31. Barnabas, L.; Ramadass, A.; Amalraj, R.S.; Palaniyandi, M.; Rasappa, V. Sugarcane proteomics: An update on current status, challenges, and future prospects. *Proteomics* **2015**, *15*, 1658–1670. [CrossRef]
32. Farinas, C.S.; Marconcini, J.M.; Mattoso, L.H.C. Enzymatic conversion of sugarcane lignocellulosic biomass as a platform for the production of ethanol, enzymes and nanocellulose. *J. Renew. Mater.* **2018**, *6*, 203–216. [CrossRef]
33. UNICA. Position on 04/12/2024 [Internet]. 2023/2024 Crop Ends as the Biggest in History. Available online: <http://www.unica.com.br/> (accessed on 8 July 2024).
34. Sugarcane Production in 2022, Crops/Regions/World List/Production Quantity/Year (Pick Lists). UN Food and Agriculture Organization, Corporate Statistical Database (FAOSTAT). 2024. Available online: <https://www.fao.org/faostat/en/#data/QC> (accessed on 8 July 2024).
35. Miranda, N.T.; Motta, I.L.; Filho, R.M.; Maciel, M.R.W. Sugarcane bagasse pyrolysis: A review of operating conditions and products properties. *Renew. Sustain. Energy Rev.* **2021**, *149*, 111394. [CrossRef]
36. Bezerra, T.L.; Ragauskas, A.J. A review of sugarcane bagasse for second-generation bioethanol and biopower production. *Biofuel Bioprod. Biorefin.* **2016**, *10*, 634–647. [CrossRef]
37. Al Arni, S. Extraction and isolation methods for lignin separation from sugarcane bagasse: A review. *Ind. Crops Prod.* **2018**, *115*, 330–339. [CrossRef]
38. Kumar, A.; Kumar, V.; Singh, B. Cellulosic and hemicellulosic fractions of sugarcane bagasse: Potential, challenges and future perspective. *Int. J. Biol. Macromol.* **2021**, *169*, 564–582. [CrossRef]
39. Reis, P.M.C.L.; Dariva, C.; Vieira, G.A.B.; Hense, H. Extraction and evaluation of antioxidant potential of the extracts obtained from tamarind seeds (*Tamarindus indica*), sweet variety. *J. Food Eng.* **2016**, *173*, 116–123. [CrossRef]
40. Israel, K.S.; Murthy, C.; Patil, B.L.; Hosamani, R.M. Study the trend in area, production and productivity of tamarind. *J. Pharmacogn. Phytochem.* **2019**, *8*, 283–289.
41. Ramesh, T.; Rajalakshmi, N.; Dhatathrean, K.S. Activated carbons derived from tamarind seeds for hydrogen storage. *J. Energy Storage* **2015**, *4*, 89–95. [CrossRef]
42. Kumar, C.S.; Bhattacharya, S. Tamarind seed: Properties, processing and utilization. *Crit. Rev. Food Sci. Nutr.* **2008**, *48*, 1–20. [CrossRef] [PubMed]
43. Gonçalves, G.R.; Gandolfi, O.R.; Bonomo, R.C.F.; Fontan, R.D.C.I.; Veloso, C.M. Synthesis of activated carbon from hydrothermally carbonized tamarind seeds for lipase immobilization: Characterization and application in aroma ester synthesis. *J. Chem. Technol. Biotechnol.* **2021**, *96*, 3316–3329. [CrossRef]
44. Nagar, C.K.; Dash, S.K.; Rayaguru, K. Tamarind seed: Composition, applications, and value addition: A comprehensive review. *J. Food Process Preserv.* **2022**, *46*, e16872. [CrossRef]
45. Contato, A.G.; de Oliveira, T.B.; Aranha, G.M.; de Freitas, E.N.; Vici, A.C.; Nogueira, K.M.V.; de Lucas, R.C.; Scarcella, A.S.A.; Buckeridge, M.S.; Silva, R.N.; et al. Prospection of fungal lignocellulolytic enzymes produced from jatoba (*Hymenaea courbaril*) and tamarind (*Tamarindus indica*) seeds: Scaling for bioreactor and saccharification profile of sugarcane bagasse. *Microorganisms* **2021**, *9*, 533. [CrossRef] [PubMed]
46. Houfani, A.A.; Anders, N.; Spiess, A.C.; Baldrian, P.; Benallaoua, S. Insights from enzymatic degradation of cellulose and hemicellulose to fermentable sugars—A review. *Biomass Bioenergy* **2020**, *134*, 105481. [CrossRef]

47. Rao, J.; Lv, Z.; Chen, G.; Peng, F. Hemicellulose: Structure, chemical modification, and application. *Prog. Polym. Sci.* **2023**, *140*, 101675. [[CrossRef](#)]
48. Khanna, P.; Sundari, S.S.; Kumar, N.J. Production, isolation, and partial purification of xylanases from an *Aspergillus* sp. *World J. Microbiol. Biotechnol.* **1995**, *11*, 242–243. [[CrossRef](#)] [[PubMed](#)]
49. Arntzen, M.Ø.; Bengtsson, O.; Várnai, A.; Delogu, F.; Mathiesen, G.; Eijssink, V.G. Quantitative comparison of the biomass-degrading enzyme repertoires of five filamentous fungi. *Sci. Rep.* **2020**, *10*, 20267. [[CrossRef](#)] [[PubMed](#)]
50. Pavlov, I.Y.; Eneyskaya, E.V.; Bobrov, K.S.; Polev, D.E.; Ivanen, D.R.; Kopylov, A.T.; Naryzhny, S.N.; Kulminskaya, A.A. Comprehensive analysis of Carbohydrate-Active Enzymes from the filamentous fungus *Scytalidium candidum* 3C. *Biochemistry* **2018**, *83*, 1399–1410. [[CrossRef](#)]
51. Weber, K.; Osborn, M. The reliability of molecular weight determinations by dodecyl sulfate-polyacrylamide gel electrophoresis. *J. Biol. Chem.* **1969**, *244*, 4406–4412. [[CrossRef](#)]
52. Voruganti, S.; Kline, J.T.; Balch, M.J.; Rogers, J.; Matts, R.L.; Hartson, S.D. Proteomic profiling of Hsp90 inhibitors. In *Chaperones*; Humana Press: New York, NY, USA, 2018; pp. 139–162.
53. Cox, J.; Mann, M. MaxQuant enables high peptide identification rates, individualized ppb-range mass accuracies and proteome-wide protein quantification. *Nat. Biotechnol.* **2008**, *26*, 1367–1372. [[CrossRef](#)]
54. Li, D.; Sun, Y.; Li, R.; Ao, T.; Liu, X.; Luo, Y. Selective conversion of corncob hemicellulose to xylose via hydrothermal treatment with Fe₂(SO₄)₃ and NaCl. *Biomass Convers. Biorefin.* **2023**, *13*, 1231–1240. [[CrossRef](#)]
55. Ravn, J.L.; Engqvist, M.K.; Larsbrink, J.; Geijer, C. CAZyme prediction in ascomycetous yeast genomes guides discovery of novel xylanolytic species with diverse capacities for hemicellulose hydrolysis. *Biotechnol. Biofuels* **2021**, *4*, 1–18. [[CrossRef](#)]
56. Li, X.; Dilokpimol, A.; Kabel, M.A.; de Vries, R.P. Fungal xylanolytic enzymes: Diversity and applications. *Bioresour. Technol.* **2022**, *344*, 126290. [[CrossRef](#)] [[PubMed](#)]
57. Alonso-Gil, S.; Parkan, K.; Kaminský, J.; Pohl, R.; Miyazaki, T. Unlocking the hydrolytic mechanism of GH92 α -1,2-mannosidases: Computation inspires the use of C-glycosides as Michaelis Complex Mimics. *Chem. Eur. J.* **2022**, *28*, e202200148. [[CrossRef](#)] [[PubMed](#)]
58. Seiboth, B.; Metz, B. Fungal arabinan and L-arabinose metabolism. *Appl. Microbiol. Biotechnol.* **2011**, *89*, 1665–1673. [[CrossRef](#)] [[PubMed](#)]
59. Janusz, G.; Pawlik, A.; Świdwerska-Burek, U.; Polak, J.; Sulej, J.; Jarosz-Wilkolazka, A.; Paszczyński, A. Laccase properties, physiological functions, and evolution. *Int. J. Mol. Sci.* **2020**, *21*, 966. [[CrossRef](#)] [[PubMed](#)]
60. Wu, T.; Jiang, Q.; Wu, D.; Hu, Y.; Chen, S.; Ding, T.; Ye, X.; Liu, D.; Chen, J. What is new in lysozyme research and its application in food industry? A review. *Food Chem.* **2019**, *274*, 698–709. [[CrossRef](#)] [[PubMed](#)]
61. Motta, M.L.L.; de Melo, R.R.; Zanphorlin, L.M.; Santos, C.A.D.; de Souza, A.P. A novel fungal metal-dependent α -l-arabinofuranosidase of family 54 glycoside hydrolase shows expanded substrate specificity. *Sci. Rep.* **2021**, *11*, 10961. [[CrossRef](#)] [[PubMed](#)]
62. Zoglowek, M.; Lübeck, P.S.; Ahring, B.K.; Lübeck, M. Heterologous expression of cellobiohydrolases in filamentous fungi—An update on the current challenges, achievements, and perspectives. *Process Biochem.* **2015**, *50*, 211–220. [[CrossRef](#)]
63. Morais, M.A.B.D.; Polo, C.C.; Domingues, M.N.; Persinoti, G.F.; Pirolla, R.A.S.; de Souza, F.H.M.; Correa, J.B.L.; Santos, C.R.D.; Murakami, T.M. Exploring the molecular basis for substrate affinity and structural stability in bacterial GH39 β -xylosidases. *Front. Bioeng. Biotechnol.* **2020**, *8*, 419. [[CrossRef](#)]
64. Harvey, A.J.; Hrmova, M.; De Gori, R.; Varghese, J.N.; Fincher, G.B. Comparative modeling of the three-dimensional structures of family 3 glycoside hydrolases. *Proteins* **2020**, *41*, 257–269. [[CrossRef](#)]
65. Rocha, V.A.L.; Maeda, R.N.; Jr, N.P.; Kern, M.F.; Elias, L.; Simister, R.; Steele-King, C.; Gómez, L.D.; McQueen-Mason, S.J. Characterization of the cellulolytic secretome of *Trichoderma harzianum* during growth on sugarcane bagasse and analysis of the activity boosting effects of swollenin. *Biotechnol. Prog.* **2016**, *32*, 327–336. [[CrossRef](#)]
66. Duarte, E.R.; Maia, H.A.R.; Freitas, C.E.S.; Alves, J.M.S.; Valério, H.M.; Cota, J. Hydrolysis of lignocellulosic forages by *Trichoderma longibrachiatum* isolate from bovine rumen. *Biocatal. Agric. Biotechnol.* **2021**, *36*, 102135. [[CrossRef](#)]
67. El Aty, A.A.A.; Saleh, S.A.; Eid, B.M.; Ibrahim, N.A.; Mostafa, F.A. Thermodynamics characterization and potential textile applications of *Trichoderma longibrachiatum* KT693225 xylanase. *Biocatal. Agric. Biotechnol.* **2018**, *14*, 129–137. [[CrossRef](#)]
68. Chutani, P.; Sharma, K.K. Concomitant production of xylanases and cellulases from *Trichoderma longibrachiatum* MDU-6 selected for the deinking of paper waste. *Bioprocess Biosyst. Eng.* **2016**, *39*, 747–758. [[CrossRef](#)] [[PubMed](#)]
69. Neumüller, K.G.; Streekstra, H.; Gruppen, H.; Schols, H.A. *Trichoderma longibrachiatum* acetyl xylan esterase 1 enhances hemicellulolytic preparations to degrade corn silage polysaccharides. *Bioresour. Technol.* **2014**, *163*, 64–73. [[CrossRef](#)] [[PubMed](#)]
70. de Souza, T.S.; Kawaguti, H.Y. Cellulases, hemicellulases, and pectinases: Applications in the food and beverage industry. *Food Bioproc. Tech.* **2021**, *14*, 1446–1477. [[CrossRef](#)]
71. Kakkar, P.; Wadhwa, N. Extremozymes used in textile industry. *J. Text. Inst.* **2022**, *113*, 2007–2015. [[CrossRef](#)]
72. Valle-Pérez, A.U.; Gómez-Angulo, J.H.; Flores-Cosío, G.; Amaya-Delgado, L. Interaction of fungal strains, biomass, and pH to produce lignocellulosic enzymes in solid-state fermentation for sustainable biotransformation of sugarcane and agave bagasse. *BioEnergy Res.* **2024**, *17*, 1015–1028. [[CrossRef](#)]

Disclaimer/Publisher’s Note: The statements, opinions and data contained in all publications are solely those of the individual author(s) and contributor(s) and not of MDPI and/or the editor(s). MDPI and/or the editor(s) disclaim responsibility for any injury to people or property resulting from any ideas, methods, instructions or products referred to in the content.